

# Cold Model Study on Melting of Ice Made by KCl Solution in Gas-Water Two-Phase Plume Area

Tao Wang<sup>1</sup>, Kanghua Pei<sup>1</sup>, Jian Zhao<sup>1</sup>, Zhao Li<sup>1</sup>, Huan Wang<sup>1</sup>, Rongwang Yang<sup>1</sup>, and Chao Chen<sup>1,a</sup>

<sup>1</sup>College of Materials Science and Engineering, Taiyuan University of Technology, 030024 Yingze West Street No. 79, Taiyuan City, Shanxi Province, P.R. China

**Abstract.** With the increasing of scrap usage in steelmaking processes, the melting of scrap becomes a very important phenomenon that limits the productivity and tap-to-tap time. Ice-water systems have been widely used to study the melting of scrap and alloys. In this study, the melting rate of saturated KCl solution ice spheres in gas-water two-phase plume zone are studied as a function of height of location, gas flowrate, and melt temperature. The results show that the shape of the ice sphere gradually changes firstly from spherical to elliptical, and finally becomes an irregular state. 1) The decreasing of the distance between the ice sphere and the bottom plugs, 2) the increasing of the gas flowrate, 3) the slightly increasing of bath temperature will all benefits the melting rate of ice spheres.

## 1 Introduction

With the international trade trend becoming more unstable, international iron ore prices continue to rise. Iron ore prices rose more than 80 per cent from April 2020 to April 2021. As a result, steel scrap has become an important national strategic resource and the main raw material for steelmaking processes. Chinese scrap consumption has increased from 83.3 million tons in 2015 to 215.93 million tons in 2019<sup>[1]</sup>. Due to economic reasons, great efforts have been made to increase the scrap usage in basic oxygen furnace (BOF) and even in secondary refining ladles. Nowadays, to the authors' knowledge, the scrap ratio in the converter steelmaking increases to more than 20%. Consequently, the melting time of steel scrap in molten steel is greatly prolonged. Besides, the mixing of chemical compositions in BOF and ladle is also delayed.

Scrap melting has been widely studied. Penz and Schenk<sup>[2]</sup> summarizes the scrap melting studies by coupled heat and mass transfer, small-scale high temperature experiments, mathematical models, and numerical simulations. Based on the similarity theory, water model studies have been widely used to study the fluid flow, mixing, and mass transfer in metallurgical reactors. A few studies were focused on the ice and water systems.

R. Vanier et al.<sup>[3]</sup> examined the weight of ice particles in water with a cooling coil in a secondary compartment. Experimental results have been obtained for heat transfer to melting ice spheres by measuring the rate of change of apparent weight.

S. Taniguchi et al.<sup>[4]</sup> studied the effect of gas injection upon the melting rate of an ice sphere in a water bath. Heat transfer coefficient was obtained from the experiment in which the melting rate of an ice sphere was measured. The

heat transfer coefficient increased with an increase in gas flow rate, while it was not influenced much by the orifice diameter and vessel shape.

J. Szekely et al.<sup>[5]</sup> concerned the rate at which ice rods melt, when immersed in a pool of water, agitated by an ascending stream of gas bubbles. The melting rate at the quiescent zone and the surface were compared.

M. Iguchi et al.<sup>[6-7]</sup> measured the velocity and turbulence around a sphere made of synthetic resin submerged in water and bubbling jets in a cylindrical vessel with bottom blowing. The effect of velocity and turbulence intensity on Nusselt number were investigated, and empirical expression for mean Nusselt number was proposed as a function of Reynolds number and turbulence intensity.

Y. L. Hao et al.<sup>[8]</sup> examined the melting and heat transfer characteristics of a fixed ice particles in flowing water. The shape changes of melting ice spheres with time and temperatures of water and at different initial ice temperature are record. The time variations of local parameters, local heat transfer coefficient and local Nusselt number at various angular positions are obtained. In addition, an empirical correlation for average Nusselt in convective melting of a solid particle is obtained.

A. K. Shukla et al.<sup>[9]</sup> studied the melting of ice samples of different geometries and sizes in an argon stirred vessel containing water. The relationships between non-dimensional groups related to heat transfer are derived for different conditions, and the heat transfer coefficient is estimated as a function of mixing power.

L. Cao et al.<sup>[10]</sup> used the ice samples with quartz sand to simulate scrap steel in BOF converter. The melting characteristics of scrap steel in the converter was studied through water model experiments.

However, in most of the water model experiments, ice

<sup>a</sup> Corresponding author: [chenchao@tyut.edu.cn](mailto:chenchao@tyut.edu.cn)

spheres or columns are the main research objects<sup>[3-9]</sup>, which can only simulate the light scrap steel with a density lighter than liquid steel. Besides, salt solutions for example KCl and NaCl solutions are used in water models to record the electro-conductivity and corresponding concentrations<sup>[11-12]</sup>. It was pointed out that the density of salt solutions is 16 to 18% heavier than water<sup>[11]</sup>. Therefore, the ice made by the denser KCl salt solution could be used to simulate the heavier scrap steel. The melting of ice made by KCl solution was rarely reported in literatures.

In this study, the melting of saturated KCl solution ice spheres in gas-water two-phase plume zone are studied for a better understanding of the melting of heavier scrap steel. The ice spheres are fixed at different locations above the plume. The shape evolution and melting rate are studied as a function of height of location, gas flowrate, and melt temperature. This study could provide theoretical basis and reference for the melting of scrap steel in the steel production process.

## 2 Experimental apparatus and procedure

Schematic diagram of the experimental device and model parameters are shown in Figure 1. and Table 1. respectively. The experiment is carried out in a cylindrical container made of plexiglass with a cubic outer vessel. The container is filled with water both inside the cylindrical vessel and outer cubic vessel. The outer cubic vessel serves to counteract the problem of light refraction when photographing the melting process of ice sphere. The air is blown by air compressor through the bottom porous plug into the vessel. The gas flow rate is controlled by the flowmeter. A gripper which is composed of iron wire is used to maintain the same height of the ice sphere. A camera is used to record the melting of the salt sphere.

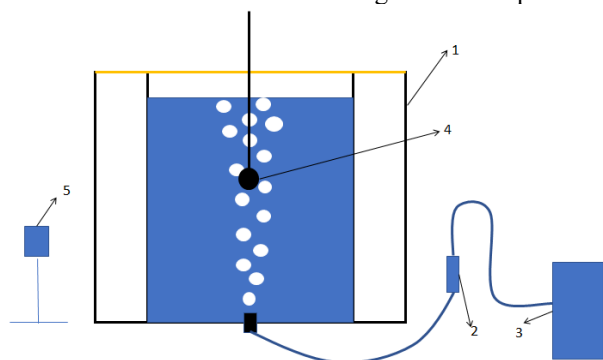


**Figure 1.** Schematic diagram of experiment devices. 1-Water model;2-flow meter;3-air compressor;4- KCl solution ice sphere;5-camera

During the experiment, the temperature of the bath was kept constant. The ice sphere was fixed at the same position. This position is precisely above the plug and the gas plume. Before the experiment, saturated KCl solution at room temperature were frozen to ice spheres in the refrigerator. The initial temperature of ice sphere was  $-24\text{ }^{\circ}\text{C}$ , and the bath temperature in this study were  $20\text{ }^{\circ}\text{C}$ ,  $25\text{ }^{\circ}\text{C}$  and  $30\text{ }^{\circ}\text{C}$  respectively. The ice spheres were placed 100mm, 200mm and 340mm above from the bottom plug location. The bottom gas flowrate increased from 0L/min

to 10L/min. After the experiment, the transverse and vertical diameters of the ice spheres were obtained through the video for intervals of 5 or 10s. The dimensionless diameter is obtained and used to analyze the melting rate of ice sphere.

**Table 1.** Water model parameters.

Water level	440mm
Diameter of cylindrical vessel	445mm
Side length of cubic vessel	600mm
Diameter of saturated KCl solution ice sphere	50mm
Diameter of porous plug	20mm

## 3 Results and discussion

### 3.1 Shape change of saturated KCl solution ice sphere in the gas-water plume

The shape variation trend of ice spheres in the gas-water plume is shown in Figure 2. During the whole melting process, the shape of the ice sphere gradually changes firstly from spherical to elliptical, and finally becomes an irregular state. As shown in Figure 3(a), when the ice sphere is fixed above the porous plug, the ice sphere is washed by bubbles. The bubbles impinging the bottom of the ice sphere and rises around the ice sphere.

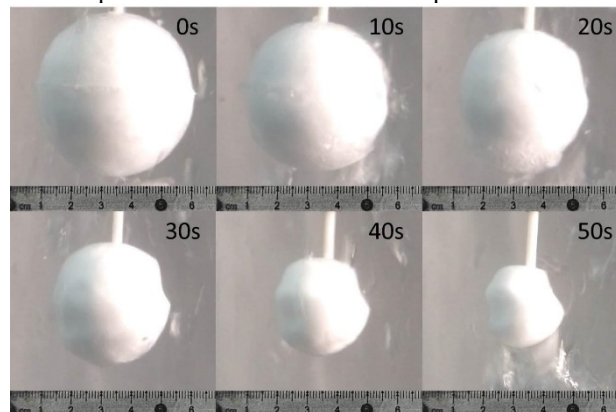


**Figure 2.** Shape of ice sphere in gas-water plume (bath temperature  $25\text{ }^{\circ}\text{C}$ , location: 200mm from the bottom, gas flow rate 3L/min)

During the melting process, a layer of crystalline delamination appears at the bottom of the ice sphere, as shown in Figure 3(b). The forced convection, mass and heat transfer of the segregated ice sphere is a complex process which maybe the reason of this phenomenon. During the freezing of ice spheres, the heavier KCl solute deposits at the bottom of the sphere and results in the segregation of KCl solute in the sphere. The mass transfer of KCl solute might be dominant at the bottom of salt ice sphere and leading to the unmelted ice layer at the bottom.

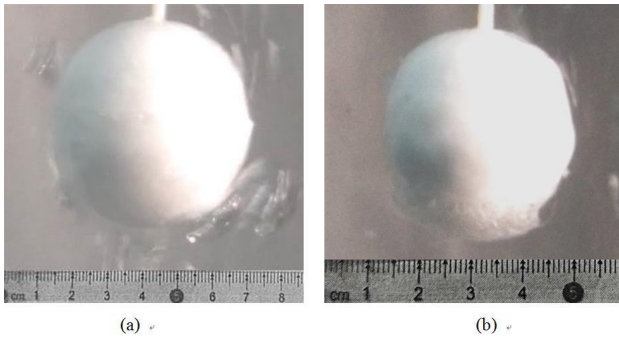


**Figure 3.** Typical shape of ice sphere melting: a- washed by air bubbles; b- stratification of ice sphere.

### 3.2 Effect of bottom blowing gas flow rate on ice sphere melting

As can be seen from Figure 4, both the transverse and vertical diameters of ice spheres as a function of time show a linear trend. The vertical diameter decreases faster than the transverse diameters for the same case. In other words, the melting rate of vertical direction is greater than that of the transverse direction. It's due to the gas washing effect for the vertical direction. Besides, the diameter change rate is gradually accelerated with the increase of bottom blowing gas flow rate.

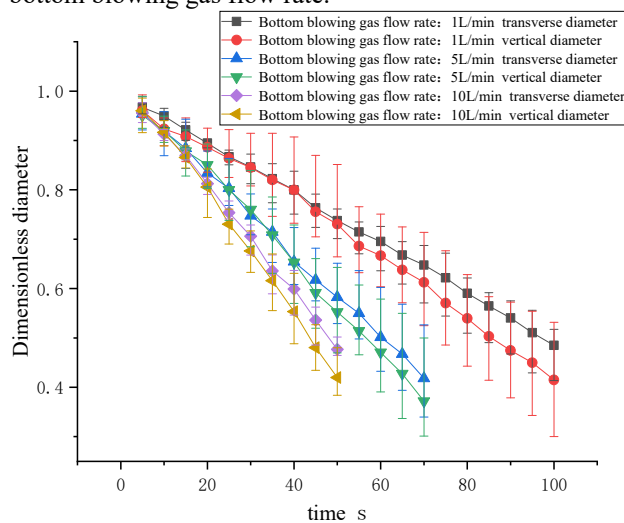


**Figure 4.** The variation of dimensionless transverse and vertical diameters of ice spheres with time for different bottom blowing flowrates (bath temperature 20°C, location: 200mm from the bottom).

After linear regression of the diameter-time curve, the rate of change of diameters are calculated and summarized in table 2. Overall, both the rate of change of transverse and vertical diameters are close to each other. The difference between the increases with the increasing of gas flow rate. For better comparison, the rate of change of the transverse diameter of the ice sphere will be used in the latter part.

**Table 2.** Comparison of rate of change of transverse and vertical diameter at different flow rates (bath temperature 20°C, location: 200mm from the bottom)

Rate of change	1L/min	5 L/min	10 L/min
----------------	--------	---------	----------

Transverse diameter(mm/s)	0.253	0.415	0.5385
Standard error	0.00883	0.4252	0.02643
Vertical diameter(mm/s)	0.276	0.446	0.6055
Standard error	0.02442	0.04619	0.04603

### 3.3 Effect of ice sphere placement on ice sphere melting

The rate of change of the transverse diameter for three locations of salt ice spheres are compared in Figure 5.

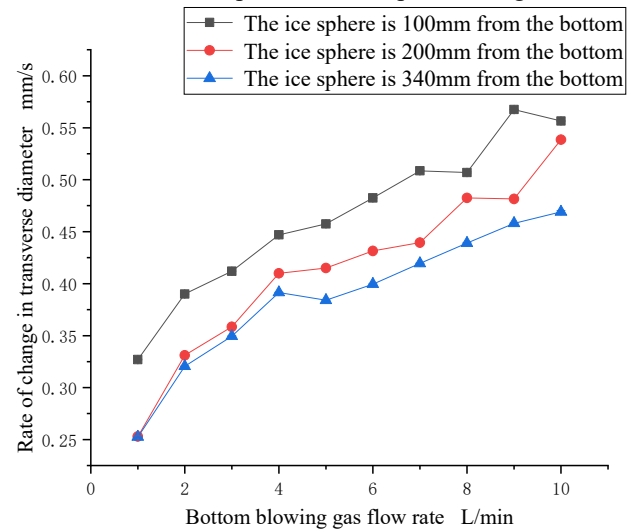


**Figure 5.** The rate of change of transverse diameters of ice spheres as a function of bottom blowing gas flow rate at different locations (bath temperature 20°C).

A general tendency could be found that the lower the locations of ice spheres the higher the melting rate. The results are not noteworthy for higher locations under small gas flowrates. As an example, the rate of change of diameter is very close for the cases that the ice sphere are 200mm and 340mm above the bottom under the gas flowrate of 1L/min to 3L/min. When the bottom-blowing gas flow rate is greater than 5L/min, the melting rates of ice spheres at these two locations are significantly different. However, the melting of ice spheres at lower position (100mm above the bottom) under the lower gas flowrate conditions is considerably higher than that at the height of 200mm and 340mm. This is due to the strong interaction between bubble plume and ice spheres. For higher gas flowrates, the bubble plume is well developed and the interaction between bubble plume and ice spheres is not significantly changed with the height of location of ice spheres. In all, the bubble plume rising, gas flowrates, and the location of ice spheres will all matters.

### 3.4 Effect of bath temperature on ice sphere melting

The effect of bath temperature on the melting rate of ice sphere is shown in Figure 6. Generally, the higher the bath

temperature the faster the melting of ice sphere. That's easy to understand as the heat and mass transfer process is accelerated. However, the results are obtained under a smaller gas flowrate, i.e. 1L/min. As described before, the melting of ice spheres at lower position (100mm) is higher than the other cases. In Figure 6, the increased temperature can slightly improve the melting of ice sphere at higher positions.

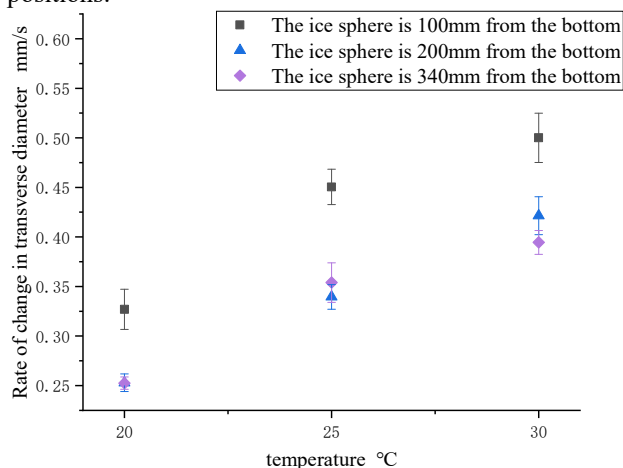


**Figure 6.** The melting rate of ice spheres at different bath temperatures (bottom blowing gas flow is 1L/min).

## 4 Conclusion

In this study, the melting rate of saturated KCl solution ice spheres in gas-water two-phase plume zone are studied as a function of height of location, gas flowrate, and melt temperature. During the whole melting process, the shape of the ice sphere gradually changes firstly from spherical to elliptical, and finally becomes an irregular state. The bubbles impinging at the bottom of the salt ice sphere will accelerate the melting process. This can be controlled by lower the height of ice sphere to the bottom gas blowing and by increasing the flowrate of gas plume. Besides, the bath temperature is playing an important role in the melting of ice sphere. Finally, the mass transfer and heat transfer mechanism of the melting of saturated KCl solution ice sphere should be paid more attention.

## Acknowledgments

The authors are grateful to the financial support of the National Natural Science Foundation of China project (51904204), Applied Fundamental Research Programs of Shanxi Province (201901D211013), Shanxi Provincial Science and Technology Major Special Project (20191102004), and undergraduate innovation and entrepreneurship training program of TYUT (20087).

## References

1. Bureau of International Recycling Ferrous Division, World Steel Recycling in Figures 2015–2019: Steel Scrap—A Raw Material for Steelmaking.
2. F.M. Penz, J. Schenk, *Steel Res. Int.* **90**, 1900124 (2019)

3. C.R. Vanier, C. Tien, *AIChE.*, **16**, 76–82 (1970)
4. S. Taniguchi, M. Ohmi, S. Ishiura, S. Yamauchi, *Trans. ISIJ*, **23**, 565-570 (1983)
5. J. Szekely, H. H. Grevet, N. EL-Kaddah, *Int. J. Heat Mass Trans.* **27**,1116-1121 (1984)
6. M. Iguchi, J.I. Tani, T. Uemur, Z. Morita, *ISIJ Int.* **29**, 658-665 (1989)
7. M. Iguchi, H. Takeuchi, H. Kawabata, T. Uemura, Z. Morita, *ISIJ Int.* **31**, 46-52 (1991)
8. Y.L. Hao, Y.X. Tao, *J. Heat Trans.* **124**, 891-903 (2002)
9. A.K. Shukla, R. Dmitry, O. Volkova, P.R. Scheller, B. Deo, *Metall. Mater. Trans. B*, **42**, 224-235 (2011)
10. L. Cao, Q. Liu, Y. Wang, W. Lin, J. Sun, L. Sun, W. Guo, *Mater. Trans.* **59**, 1829-1836 (2018)
11. C. Chen, G. Cheng, H. Sun, Z. Hou, X. Wang, J. Zhang, *Steel Res. Int.* **83**, 1141-1151 (2012)
12. C. Chen, Q. Rui, G. Cheng, *Steel Res. Int.* **84**, 900-907 (2013)